RSC Advances

ROYAL SOCIETY OF CHEMISTRY

www.rsc.org/advances

Methanol tolerant, high performance, noble metal free electrocatalyst educed from Polyaniline and Ferric chloride for Oxygen reduction reaction

SankararaoMutyala[a], JayaramanMathiyarasu*[a],Ashok Mulchandani[b]

[a]*Electrodics and Electrocatalysis Division, CSIR-Central Electrochemical Research Institute, Karaikudi 630003, India. E-mail; al_mathi@yahoo.com*
[b]*Department of Chemical and Environmental Engineering, University of California, Riverside, CA 92521, USA*

Development of low cost oxygen reduction catalysts with improved performance is required for the commercial success of eco-friendly energy conversion systems. Here in, we report a facile and controllable chemical route for the synthesis of porous *iron-nitrogen-carbon* (Fe-N-C) cathode catalyst for oxygen reduction reaction (ORR). The catalyst is prepared by pyrolysis of polyaniline (PANI) with ferric chloride in a tubular furnace at 800 ^{o}C in an inert atmosphere. The structural and morphological features of resultant catalysts are fully characterized by spectroscopic and microscopic techniques. The electrocatalytic activities were demonstrated by linear sweep voltammogram (LSV) and chronoamperometric measurements. According to rotating disc electrode (RDE) measurements and Koutecky-Levich analysis porous Fe-N-C architecture possesses surpassing electrocatalytic activity for ORR via a virtual four electron transfer pathway. Compared to commercial Pt/C (20 wt. % E-Tek) catalyst, the synthesized Fe-N-C catalyst exhibited 25 mV cathodic shift with a close kinetic current density. The present catalyst exhibited methanol tolerance characteristics which are superior to the commercial Pt/C catalyst. This behaviour is reasoned as the existence of numerous active sites of nonporous iron, which is exposed at the catalyst surface with porous structure of large surface area. Thus, the present Fe-N-C catalyst may be employed as an efficient and inexpensive noble metal-free ORR catalyst for fuel cell applications.

Introduction

Fuel cells, particularly, the proton-exchange membrane (PEMFCs) and direct methanol fuel cells (DMFCs) have been considered as one of the promising devices for clean, green and efficient energy conversion systems for the near future. However, the sluggish ORR kinetics on cathode requires high Pt loading which in-turn increases cost of the devices that limits the future large-scale commercial applications of DMFCs/PEMFCs[1-4]. Mostly, Pt and Pt based alloys have been used as most efficient catalysts for ORR; however, it is too expensive, lacking of methanol tolerance and less abundance, remain the key challenges to widespread commercialization[5]. Therefore, replacement of Pt-based catalysts with inexpensive catalysts may be a preferred way to improve the application of fuel cells. One of the non-noble metal alternatives to Pt is heteroatom-doped carbon nanomaterials, which exhibit high ORR performance with good stability in an alkaline medium[6-8]

Concurrently, nitrogen doped carbon (NDC) materials and polyaniline derived metal free carbon materialsare also considered to be a possible aspirant for Pt to reduce the cost and enhance the catalytic activity for ORR[9-13]. The incorporation of nitrogen atom into carbon network endows them with unique electronic properties due to conjugation between nitrogen lone-pair electrons and carbon 'π' system and thus considerably enhances the number of active sites for ORR[14]. It is proposed that the inherent active sites for ORR in NDC materials might include pyridinic, pyrrolic and graphitic nitrogen species. Among them, graphitic and pyridinic nitrogen are regarded as the prospective ORR active sites[15,16].Synthesis of carbon materials with rich in graphitic nitrogen content requires high formation energy. Also, the mild synthetic conditions resulted in the formation of predominantly pyrrolic nitrogen which is of less attractive for ORR reaction[17]. Therefore, it is of ideal to synthesize NDC with rich in graphitic and pyridinic nitrogen content for better ORR activity. However, when compared to Pt based catalyst the performance of NDC towards ORR activity is less competitive.

As another kind of non-noble metal based-electrocatalysts, the combination of NDC materials with trace amount of transition metal may be a desired way to promote ORR activity efficiently[18,19]. In the past decades, transition metals incorporated conducting carbon materials are widely used as alternative catalysts for ORR in alkaline medium, due to their abundance and environmental compatibility[20].Literature information indicates that the introduction of trace amount of transition metal could effectively increase the activity of NDC materials. Thus, considering both NDC material and transition metal having considerable ORR activities, it will be attractive to study the ORR performance of their composites.

Hence, it is necessary to develop new strategies for the improvement of ORR activity of NDC materials.To overcome aforementioned issues, here in we report a high-performance porous Fe-N-C catalyst for ORR in an alkaline medium. This catalyst is partially graphitized and prepared by simple carbonization process. Among the various synthesized catalysts, Fe-N-C catalyst showed admirable performance for ORR in alkaline medium and comparable to conventional Pt/C catalyst in terms of ORR kinetic current density. Therefore, it is encouraging and interesting to investigate the ORR of synthesized Fe-N-C catalysts. The advantages of the synthesized catalyst are showing excellent performance for ORR, cost-effective and serve as good cathodic catalyst for fuel cell application.

Experimental Section

Chemical

The following chemicals are received and utilized without further purification. Chloroform, potassium hydroxide, hydrochloric acid and aniline were obtained from Merck. Ammonium peroxydisulfate (APS) and ferric chloride ($FeCl_3$) are received from Alfa Aesar. 20 wt. % Pt/C was purchased from E-Tek. Nafion (5 wt. %) was purchased from Sigma-Aldrich. Throughout the experiments, solutions were prepared using Millipore water of 18.2 MΩ cm resistivity.

Preparation of catalysts

PANI was synthesized by a conventional chemical route. Briefly, 0.2 M aniline hydrochloride and 2.5 M APS were rapidly mixed together in water and allowed to stand for 24 h for complete polymerization. The resulted solids were separated by filtration, washed thoroughly with acetone followed by water and dried under vacuum for 4 h at 70^{o}C to obtain green powder of PANI. Whereas, 0.05 M $FeCl_3$was introduced along with aniline and the above procedure was followed for PANI+Fe material preparation. Here, $FeCl_3$ is metal precursor and PANI is the only precursor for both carbon and nitrogen. Carbonization of PANI and PANI+Fe catalyst was carried out in a programmable tubular furnace (Thermo make) where the temperature has increased at a rate of 1 ^{o}C s^{-1} upto 800^{o}C and maintained 1 h at this temperature in an inert atmosphere. After

carbonization, the sample was allowed to cool at ambient room temperature that resulted NDC and Fe-N-C materials respectively.

Fabrication of catalyst modified Glassy Carbon electrodes

Glassy carbon electrode (GCE) was polished carefully using 0.3 and 0.05 μm alumina pads, then sonicated in water and absolute ethanol. The catalyst ink was prepared as briefly; 2 mg of synthesized catalyst or Pt/C was dispersed in 1 mL of water and 5 μL of Nafion (0.5 wt. %) by 30 min sonication. The catalyst layer was prepared by drop cast 5 μL of catalyst ink on gutted GC electrode surface using a micropipette and dried at room temperature.

Structural characterization

The physical properties of the derived catalysts were examined using X-ray photoelectron spectroscopy (XPS) that was carried out with Multilab 2000 Thermo scientific (UK) X-ray photoelectron spectrometer. Mg Kα X-ray (1253.6 eV) with 200 W power was used as the exciting source and 10 eV energy pass was used for data collection. The energy analyzer employed was a hemispherical analyzer of 150 mm diameter. The vacuum maintained during the experiment was 10^{-10} mbar. Experimental data were curve fitted using Shirley background with a Gaussian and Lorentzian mix product function. Scanning electron microscope (SEM) characterization was carried out using Model Zeiss Ultra 55 operated at an accelerating voltage of 5 kV to study the surface morphology of the synthesized materials. The elemental composition (CHN) analysis was recorded using Elementarvario EL III, German. High Resolution Transmission Electron microscopy (HR-TEM) analysis was carried out using Tecnai Netherlands. Raman spectra were recorded using high resolution dispersive Renishaw make Laser Raman spectrophotometer employing Helium-Neon excitation Laser of maximum power density 2.0 watts (632.8 nm). X-ray diffraction (XRD) measurements of the synthesized catalysts were carried out on a Philips PAN analytical PRO X-ray diffractometer using Ni-filtered Cu Kα radiation (λ = 0.15406 nm). The XRD patterns were obtained in a step-scanning mode with narrow receiving slit (0.5°) of counting time 15 s/0.1°. The identification of phases was made by referring to the Joint Committee on Powder Diffraction Standards International Center for Diffraction Data database.

Electrochemical measurements

A three-electrode configuration was used, with a catalyst layer modified GC electrode as working electrode; platinum wire and Ag/AgCl (in saturated KCl solution) as counter and reference electrodes respectively. The ORR activities of the catalysts were evaluated by linear sweep voltammetry (GC electrode with diameter of 3.0 mm), rotating disc electrode (RDE) experiments performed in oxygen saturated 0.1 M KOH solution at a scan rate of 0.01 Vs^{-1} and chronoamperometry method is used for methanol tolerance studies. All these experiments were carried using Potentiostat/Galvanostat BAS 100B (Bioanalytical Systems Inc.) /Autolab (Ecochemie) electrochemical work station at room temperature (25±1°C). LSV experiments were conducted under oxygen saturated 0.1 M KOH electrolyte, at a scan rate of 0.01 Vs^{-1}. All potentials showed in this work are against Ag/AgCl reference electrode and during this study commercial Pt/C catalyst 20% (E-Tek) was used for comparison. Capacitive current measurements were carried out using cyclic voltammetric (CV) measurement in 0.1M KOH at 10 mV/s sweep rate in the potential range -0.8 to 0.2 V *vs* Ag/AgCl.

Results and discussion

The preservation of morphological features of synthesized PANI even after the carbonization process is well established in our previous work and by other researchers[21,22]. After heat treatment at 800°C for 1 h in an inert atmosphere, the porous morphology was retained and only some agglomerations are observed for PANI as shown in Fig.1A. When iron is introduced in the NDC materials that also retained the porous structures with smaller amount of iron particle incorporation in the NDC material, is clearly observed in Fig. 1B. In addition Fig. 1C& D shows the representative HR-TEM images of NDC and Fe-N-C materials respectively. The HR-TEM image of Fe-N-C material confirms the present of iron particles with a typical size of 30-40 nm embedded over the NDC. The schematic diagram for NDC and Fe-N-C catalysts preparation procedure are exhibited in scheme.1. The carbonization process is allied with the mass loss for practical applications. The yield in the carbonization process in air is low; i.e. below 10 wt %, [23]but in an inert atmosphere weight loss is close to 30 % [24]. In this work 26 % weight loss is observed during the carbonization process. The yield decreases with increase in carbonization temperature and better conversion of the molecular structure is expected at higher temperature[25]. Further, spectroscopic and diffraction studies are employed to identify the structural vicissitudes. The changes in elemental composition are not large, but the proportion of nitrogen and carbon atoms significantly decreases. Considerable changes in the molecular structure are reflected in Raman spectroscopy and XPS analysis.

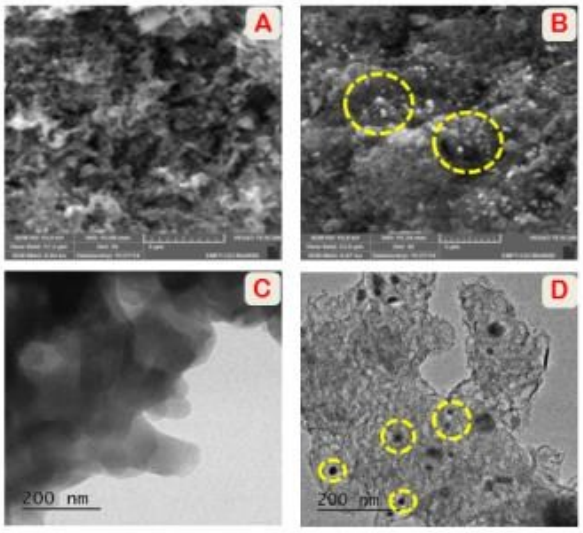

Fig.1 SEM images of (A) NDC (B) Fe-N-C materials and HR-TEM images of (C) NDC (D) Fe-N-C materials

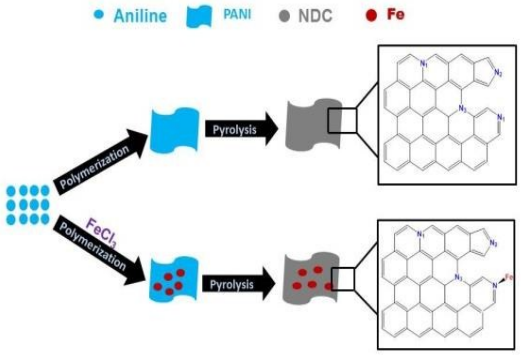

Scheme.1 Schematic representation of NDC and Fe-N-C materials synthesis process

X-ray diffraction study

The architecture of synthesized NDC and Fe-N-C materials are characterized by XRD. Fig. 2A shows wide angle powder XRD pattern of respective materials. Here, NDC material exhibits a broad peak at 2θ value of 24.48, corresponds to carbon lattice with 0.36 nm interlayer distances, which is indexed (002) plane, resembles graphitic lattice. However, pristine graphitic carbon has (002) plane at 2θ value around 26.5 with 0.33 interlayer distances between the graphitic carbon sheets. The carbon sheets interlayer distance for NDC is marginally higher than pure graphitic carbon. This could be due to structural changes and partial graphitization of carbon network during carbonization of PANI. Similar results are reported on some partially graphitic mesoporous carbon materials[26]. In addition, NDC materials also show a broad reflection peak at 2θ = 43.5° corresponds to superposition of (101) plane reflections of the graphitic carbon and strongly attest a higher degree of carbonization. This result confirms that partially graphitic structure was successfully obtained from carbonized PANI at 800°C. It is described that preparation of porous carbon materials with graphitic carbon nature using carbon sources such as sucrose and furfuryl alcohol is very difficult if the carbonization temperature is lower than 1100°C[27]. Thus, it is reasonable to assume the formation of highly graphitic carbon due to the aromatic carbon as the precursor and the phenyl group attached to an amino group.

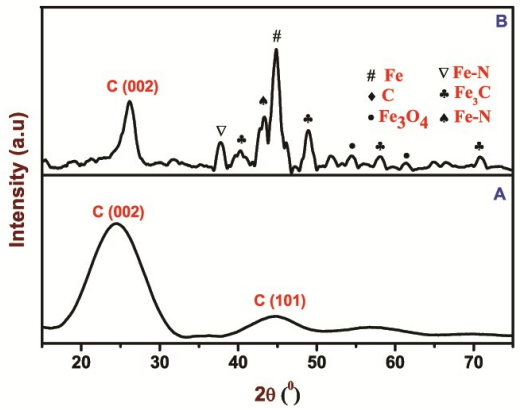

Fig.2 Shows the XRD pattern of (A)NDC and (B)Fe-N-C materials

XRD pattern of Fe-N-C material andposition of the diffraction lines are encompassed in Fig.2B. It can be seen that the catalyst exhibited sharp diffraction peak at 24.4° which is indexed as (002) plane, strongly reflect the feature of graphitic carbon. In addition, the apparent diffraction features of Fe-N-C catalyst were also observed due to small Fe loading into NDC. Based on the amount of Fe loading, the main diffraction peak observed at 2θ = 44.6° intends to the possible existence of the crystalline planes of metallic iron (JCPDS File no 01-072-1110). The remaining diffraction peaks are attributed to characteristics of Fe_3O_4, Fe-N and Fe_2N phases. As a result, XRD patterns indicate that Fe-N-C catalyst composed of a mixture of Fe_3O_4, Fe-N and Fe_2N along with metallic Fe phases. It should be noted that chemical structures of Fe are obviously different from NDC, since different forms of iron, to the extent possible are exhibited in the XRD patterns. Moreover, some Fe species could be scarcely identified by using XRD due to the presence of amorphous phase and it is also good in agreement with SEM studies. Accordingly, additional XPS, and Raman analyses are carried out to further explore the chemical environment of nitrogen, the coordination geometry, and bonding of its local environment around the Fe atoms.

Raman Spectroscopy

Raman spectroscopy analysis was carried out to study the structural changes in the carbon architecture. Fig.3 shows the normalized Raman spectra of synthesized catalysts in 500-2000 cm^{-1} region collected using laser of 632.8 nm emission. The spectra of the pristine PANI, PANI+Fe and NDC are also exhibited for the sake of comparison. PANI, PANI+Fe, NDC and Fe-N-C materials exhibited characteristic peak at around 1575 cm^{-1} (G-band) corresponds to E_{2g} mode of sp^2 carbon. In addition, PANI exhibited the D band at 1476 cm^{-1}, however after addition of Fe and carbonization process, the D-band shifted to 1354 cm^{-1} strongly equates to disordered nature of carbon material. The intensity ratio of D and G bands (I_D/I_G) calculated, is used to infer the degree of graphitization in the carbon materials. The decrease in (I_D/I_G) ratio clearly signifies the enhanced graphitization. The creation of structural changes in the presence of iron is further supported by XPS analysis.

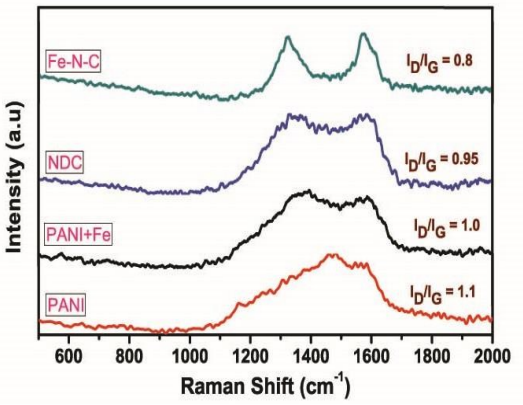

Fig.3 Raman spectra of respective materials.

XPS characterization

X-ray photoelectron spectroscopy (XPS) characterization was carried out to explore the surface elemental composition of nitrogen and iron doped carbon materials. Figure 4A shows the high resolution C1s spectra of NDC and Fe-N-C materials. The deconvolution of C1s main signal of Fe-N-C shows two predominant peaks with a binding energy of 284.8 (65.9%) and 285.5 (19.9 %) eV, assigned to sp^2 (graphitic) and sp^3 (diamond)[28]like carbon respectively with a sp^2:sp^3 of 3.3:1. Several other small peaks are also observed at 286.6 (9.5 %), 286.9 (2.1 %) and 288.2 (2.2 %) eV corresponds to C-O, C-N and C=O bonds respectively[29, 30]. The C1s spectra of NDC sample also exhibited similar peaks of sp^2 and sp^3 carbon where the ratio is found to 1.4:1.0 indicated poor graphitic value. In both, the predominant C1s peak centred at 284.8 eV and its asymmetric pattern is due to the presence of C-N bond in the carbon lattice, which indicates nitrogen atoms are successfully incorporated into the carbon network during carbonization[31].

Fig. 4B shows the N1s spectrum of NDC and Fe-N-C materials. The deconvolution of N1s spectra of NDC material showed four peaks at 398.2, 399.7, 401.0 and 402.2 eV, which are assigned to pyridinic N (22.8%), pyrrollic N (28.15%), graphitic N (46.34%) and oxidized form of nitrogen (2.65%) respectively. The deconvoluted N1s spectra of Fe-N-C material also exhibited all the above nitrogen peaks, but interestingly with an improved graphitic N value of 63.5%. The improvement in the graphitic N percentage warrants high ORR activity[32]. In addition, the peak observed at 399.0 eV strongly corresponds to the presence of N-Fe bonding, which clearly confirms the formation of Fe-N bonding in Fe-N-C material. Incorporation of iron in carbon

network could be responsible for the catalytic conversion in the form of graphitic carbon[33].

Fig.4C shows the deconvoluted Fe2p spectrum of Fe-N-C material and it results six peaks viz. 709.7, 710.7, 711.5, 712.6, 713.6 and 719.2 eV. The set of bands observed for Fe is due to the formation of iron in different oxidation states[32, 34]. The peaks appeared at 709.7 eV and 710.7 eV corresponds to $2p^{3/2}$ of Fe (II) ion and Fe (III) ion respectively[34, 35]. The peaks at 713.6 and 719.2 eV are the satellite peaks of Fe (II) and Fe (III) respectively and it clearly confirms the co-existence of Fe (II) and Fe (III) in this material. The peak area calculated indicated the relative abundance of iron and its composites in the Fe-N-C material as shown in Table.1. Therefore, the present observation clearly confirms the formation of Fe-N bond together with C-N bond in the Fe-N-C material that plays a crucial role in improving the ORR performance.

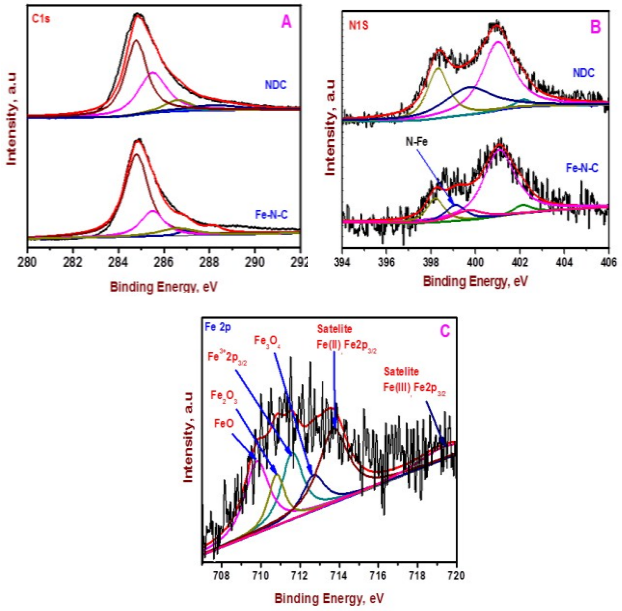

Fig.4 Deconvoluted high resolution (A) C1s XPS spectra, (B) N1s XPS spectra of respective materials (C) Fe2p spectra of Fe-N-C material. Inset indicates the respective composite and states of iron.

Electrocatalytic activity of synthesized catalysts

The electrocatalytic activity of the synthesized materials towards ORR was investigated by voltammetric studies in oxygen saturated 0.1 M KOH solution. From electrocatalytic point of view PANI and PANI-Fe materials are poorly active towards ORR in alkaline medium. However, after carbonization remarkable increase in electrochemical activity was noticed and Fe incorporation in NDC material exhibited enhanced ORR activity in alkaline media. The ORR activity of the synthesized materials is compared with the commercially available catalyst Pt/C 20% (E-Tek) supported on a GC electrode.

Fig.5 shows the comparison linear sweep voltammograms of the ORR activity of (a) PANI, (b) PANI+Fe (c) NDC (d) F-N-C and (e) Pt/C catalysts. From the figure, it is observed that the ORR activity improved to a greater extent when nitrogen is introduced in the carbon network. For instance, the onset potential of PANI and PANI+Fe is found to be - 0.345 V whereas in the case of NDC the potential has shifted to - 0.25 V, i.e., 95 mV anodic shift was observed. Comparison of electrochemical reduction of oxygen between Fe-N-C and NDC reveals that the addition of trace amount of Fe into NDC greatly promote the ORR activity. The onset potential of ORR at Fe-N-C is found to -0.04 V which is more positive than NDC and PANI/PANI-Fe. The voltammetric current density for ORR on Fe-N-C (4.6 $mAcm^{-2}$) is three times higher than PANI (1.53 $mAcm^{-2}$). The enhanced activity in Fe-N- C catalyst, suggests that Fe-N-C catalyst has a large surface area compared to PANI, PANI+Fe and NDC, which is revealed by quantifying the capacitive current measurements (supporting information S1). This is due to the interconnected pores in Fe-N-C material that increases the active sites and effectively improves the electrochemical performance. It is reported that single iron atom cannot effectively transfer electrons to the oxygen molecule. Instead, the neighboring atom or group of atoms facilitates ORR on the pyrolyzed catalysts[36-38].The performance of Fe-N-C is compared with the commercial Pt/C 20% (E-Tek) catalyst (-0.015 V onset potential), which revealed that the Fe-N-C catalyst exhibited a close performance in terms of ORR onset potential and current density with the Pt catalyst. The large discrepancy in the activity between NDC, PANI/PANI-Fe and Fe-N-C is due to the availability of active sites which are exposed to the porous Fe-N-C catalyst surface for ORR. The combination of trace amount of Fe incorporation in the NDC matrix along with porous structural architecture contributes an enhanced ORR activity of Fe-N-C material.

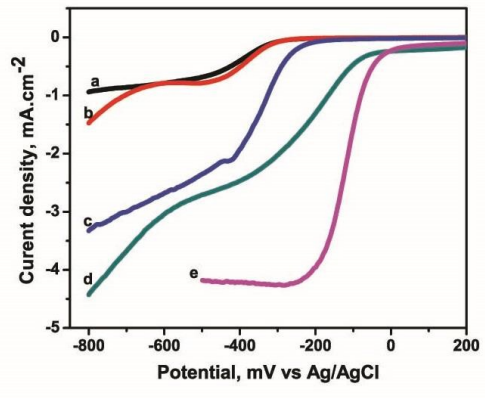

Fig.5 Comparison LSV curves of ORR at (a) PANI, (b) PANI+Fe (c) NDC (d) F-N-C and (e) Pt/C catalysts modified GC electrodes in an oxygen saturated 0.1 M KOH aqueous solution (Scan rate $0.01Vs^{-1}$: at 1600 rpm).

From the above LSV analysis Fe-N-C material showed enhanced activity towards ORR and its performance is close to commercial Pt/C 20% (E-Tek) catalyst. In further, rotating disk electrode (RDE) experiments are carried out to investigate the kinetic parameters of Fe-N-C catalyst towards ORR. In order to understand the catalytic mechanism, LSV curves of Fe-N-C samples (Fig.6A) were recorded in O_2 saturated 0.1 M KOH electrolyte at different rotation rates. From the figure, it is observed that the reduction current is found to increase with the rotation rate. The number of electron transferred (n) per oxygen molecule in the ORR process is calculated by Koutechy-Levich (K–L) equation[39]

$$\frac{1}{i}=\frac{1}{i_k}+\frac{1}{i_d} \quad =\frac{1}{i_k}+\frac{1}{0.2nFD_o^{2/3}\omega^{1/2}\upsilon^{-1/6}C_o} \quad =\frac{1}{i_k}+\frac{1}{B\omega^{1/2}} \qquad [1]$$

where i_k is kinetic current density, B is Levich slope, n is the number of electrons involved in ORR process per O_2 molecule, C is the saturation concentration of oxygen in electrolyte (1.1×10^{-6}mol/L), D is the diffusion coefficient (1.9×10^{-5} cm^2 s^{-1}), υ is the kinematic viscosity of solution (1.0×10^{-2} cm^2 s^{-1})[40] and ω is the rotation rate in rpm. The K-L equation relates the current density (i) to rotation rate of the electrode (ω). A plot of j^{-1} vs $\omega^{-1/2}$ should give parallel straight lines at different applied potentials is showed in Fig.6B. Fe-N-C catalyst showed linearity and parallelism, confirming that ORR follows first-order kinetics

with respect to O_2 molecule. Further, the plots do not pass through the origin, indicating a mixed kinetic-diffusion-controlled mechanism[41]. The number of electrons involved in the ORR calculated using K-L equation works out to ~ 3.8. This observation revealing that the electrocatalytic process of ORR at Fe-N-C catalyst is close to four-electron pathway leading to the direct formation of OH^-. Thus, the possible ORR mechanism may be given as follows:

$$O_2 + 2H_2O \xrightarrow{4e-} 4OH^- \qquad [2]$$

The above observation with enhanced electrocatalytic activity of Fe-N-C modified GC electrode towards ORR is due to formation of new carbon structure during carbonization and improved porous surface area.

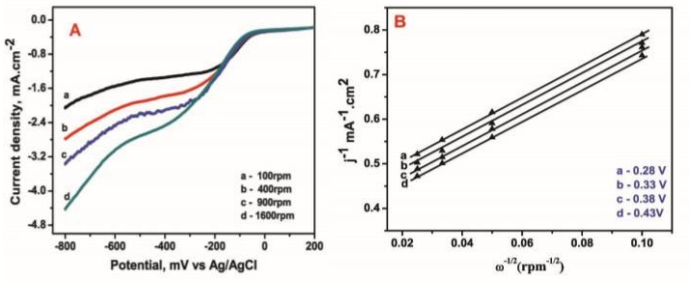

Fig.6 (A) RDE voltammograms of Fe-N-C modified GC electrode in an O_2saturated, 0.1 M KOH solution at a scan rate of 0.01V s^{-1} atdifferent rotation rates (B) K–L plots for ORR at different electrode potentials for Fe-N-C.

Methanol tolerance Effect

The methanol tolerance ability for a cathode material is an important issue in alcohol fuel cells[45]. Fig.7 shows the chronoamperometric response of (a) Fe-N-C and (b) Pt/C modified GC electrodes with the addition of 2 M methanol in 0.1 M KOH solution. The Fe-N-C catalyst almost unaffected even after the addition of high concentration of methanol, conversely the corresponding current observed on the commercial Pt/C shifted from cathodic to anodic current region within a short period, indicating a conversion of the dominated ORR process over the methanol oxidation reaction. This result suggests that Fe-N-C catalyst is completely resistant to methanol oxidation / adsorption. This observation is very much important in the context of direct methanol fuel cell applications. The above development expected the utility of this Fe-N-C as a methanol tolerant ORR catalyst in alkaline fuel cell configuration that offers a competitive advantage over the *state-of-the-art* conventional Pt/C materials.

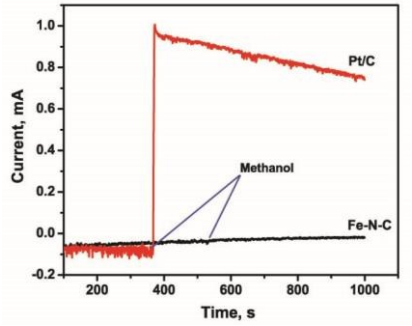

Fig.7 Chronoamperometric responses of Pt/C and Fe-N-C catalysts at -0.15 V vs Ag/AgCl in O_2saturated 0.1 M KOH electrolyte

ORR Stability Characterization

Another major concern in developing electrocatalysts is their durability in fuel cell performance. Normally carbon supported catalyst materials are suffered from a durability concerns due to weak interaction between carbon and metal atom. The use of nitrogen doping is expected to increase the bonding energy of the metal with the carbon support[42-43]. According to density functional theory, various nitrogen arrangements in carbon network have a positive effect on the binding energy, showing an increase in activity[44]. Based on these observations the present Fe-N-C catalyst is expected to have a better interaction between Fe ion and N that should be strong enough to give a durable activity of Fe-N-C for ORR. Thus, Fig.8 shows the durability test of Fe-N-C and Pt/C 20% (E-Tek) catalysts. LSV curves were recorded for these catalyst materials up to 2000th cyclein O_2saturated 0.1 M KOH solution at 1600 rpm.The catalyst's durability is assessed in terms of degradation in their half-wave-potential ($E_{½}$) after 2000 cycles[46]. The Fe-N-C catalyst exhibited only 5 mVdegradation whereas Pt/C catalyst (Fig.8B) showed 42mV negative shift. Thus, the surface properties of the non-precious metal catalyst are maintained during the potential cycling test. This information clearly indicated that the synthesized material is more durable than the Pt/C 20% (E-Tek) for fuel cell applications.

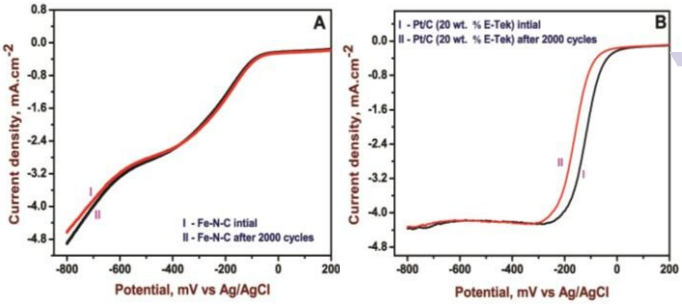

Fig.8 Comparison of LSV curves for (A) Fe-N-C, (B) Pt/C catalysts for ORR on (I) initial and (II) after 2000 cycles in O_2 saturated 0.1 M KOH at 1600 rpm with the sweep rate of 10 mVs^{-1}.

Conclusion

In summary, we have synthesised a series of catalysts by pyrolyzing PANI supported ferric chloride at 800^{o}C in an inert atmosphere and they readily transferred onto various substrates. The high-quality catalysts were characterized and evidenced by Raman, XRD, SEM and XPS measurements. Based on XPS and voltammetric results, it is speculated that high surface area and N-Fe bonds incorporated into the carbon matrix are responsible for ORR active sites. The Fe-N-C catalyst showed improved performance for ORR in alkaline medium compared to PANI, PANI+Fe, NDC. The catalytic current density at the Fe-N-C modified GC electrode was found to be *three* times higher than PANI and close performance to the commercial Pt/C catalyst. Thus, Fe-N-C catalyst is demonstrated to have best ORR activity and a preferred catalyst material for a direct four-electron reduction pathway. In addition to high ORR activity, the as-prepared Fe-N-C catalyst shows superior methanol tolerance and durability compared to commercial Pt/C. It is notable that the Fe-N-C possesses remarkable electrocatalytic properties for ORR with methanol tolerance and durability character;so it could be a promising candidate as a cathode catalyst in a fuel cell configuration.

Acknowledgements

The authors gratefully acknowledge Dr. Vijayamohanan K Pillai, Director, CECRI, for his constant encouragement. JM greatly acknowledges Raman Research fellowship [22/RRF/2012-ISTAD dt. 12.3.2013] by Council of Scientific Industrial Research (CSIR), New Delhi, India. SM greatly acknowledges CSIR, New Delhi for awarding a Senior Research Fellowship.

Notes and References

1 G. Gupta, D. A. Slanac, P. Kumar, J. D. W. Camacho, J. Kim, R. Ryoo, K. J. Stevenson and K. P. Johnston, *J. Phys. Chem. C*. 2010, **114**, 10796.
2 S. H. Liu, C. C. Chiang, M. T. Wu and S. B. Liu, *Int. J. Hyd. Ener*. 2010, **35**, 8149.
3 S. H. Liu, S. C. Chen and W. H. Sie, *Int. J. Hyd. Ener*. 2011, **36**, 15060.
4 D. Z. Mezalira and M. Bron, *J. Power Sources*. 2013, **231**, 113.
5 H. A. Gasteiger and N. M. Markovic, *Science*.2009, **324**, 48.
6 H. Jiang, Y. Zhu, Q. Feng, Y. Su, X. Yang and C. Li, *Chem. Eur. J*. 2014, **20**, 3106.
7 J. P. Paraknowitsch and A. Thomas, *Energy Environ. Sci.* 2013, **6**, 2839.
8 Y. Zhang, X. Zhuang, Y. Su, F. Zhang and X. Feng *J. Mater. Chem.A*. 2014, **2**, 7742.
9 D. Geng, Y. Chen, Y. Li, R. Li, X. Sun, S. Ye and S. Knights, *Energy Environ. Sci*. 2011, **4**, 760.
10 S. Shanmugam and T. Osaka, *Chem. Commun*. 2011, **47**, 4463.
11C. Jeyabharathi, P. Venkateshkumar, S. Mutyala, J. Mathiyarasu and K. L. N Phani, *ElectrochimicaActa*. 2012, **74**, 171.
12 K. Wan, Z. Peng, and Z. X. Liang, *Catalysts.* 2015, **5**, 1034.
13 R. Silva, D. Voiry, M. Chhowalla and T. Asefa, *J. Am. Chem. Soc*, 2013, **135**, 7823.
14 J. Liang, Y. Jiao, M. Jaroniec and S. Z. Qiao,*Angew. Chem. Int. Ed*. 2012, **51**, 11496.
15 P. Wang, Z. Wang, L. Jia and Z. Xiao, *Phys. Chem. Chem. Phys*. 2009, **11**, 2730.
16 H. Kim, K. Lee, S. I. Woo and Y. Jung, *Phys. Chem. Chem. Phys*. 2011,**13**, 17505.
17 J. Wang, G. Wang, S. Miao, X. Jiang, J. Li and X. Bao, *Carbon*. 2014, **75**, 381.
18 H. W. Liang, W. Wei, Z. S. Wu, X. Feng and K. Mullen, *J. Am. Chem. Soc.* 2013, **135**, 16002.
19 S. Jiang, C. Zhu and S. Dong, *J. Mater. Chem. A.* 2013, **1**, 3593.
20Y. Su, H. Jiang, Y. Zhu, X. Yang, J. Shen, W. Zou, J. Chen and C. Li, *J. Mater. Chem. A.* 2014, **2**, 7281.
21S. Mutyala and J. Mathiyarasu, *Int. J. Electrochemistry*. 2014, 246746.
22 M. M. Yang, B. Cheng, H. H. Song and X. H. Chen, *Electrochim.Acta*. 2010, **55**, 7021.
23 M. Trchova, P. Matejka, J. Brodinova, A. Kalendova, J. Prokes and J. Stejskal, *Polym.Degrad. Stab*. 2006, **91**, 114.
24 M. Trchova, E. N. Konyushenko, J. Stejskal and J. Kovarova, *Polym.Degrad. Stab*. 2009, **94**, 929.
25 Z. Rozlivkova, M. Trchova, M. Exnerova and J. Stejskal, *Synthetic Metals*. 2011, **161**, 1122.
26Y. Xia and R. Mokaya, *Adv. Mater*. 2004, **16**, 1553.
27 S. H. Joo, S. J. Choi, I. Oh, J. Kwak, O. Terasaki and R. Ryoo, *Nature*. 2001, **412**, 169.
28 M. Castellino, V. Stolojan, A. Virga, M. Rovere, K. Cabiale and A. Gallon, *Bioanal Chem.* 2013, **405**, 321.
29 Z. L. Hu, M. Aizawa, Z. M. Wang, N. Yoshizawa and H. Hatori, *Langmuir*. 2010, **26**, 6681.
30 S. M. Lyth, Y. Nabae, S. Moriya, S. Kuroki, M. A. Kakimoto, J. I. Ozaki, *J. Phys. Chem. C*. 2009, **47**, 20148.
31 Q. Liu, H. Zhang, H. Zhong, S. Zhang and S. Chen, *ElectrochimActa*. 2012, **30**, 313.
32 T. Choudhury, S. O. Saied, J. L. Sullivan and A. M. Abbot, *J. Phys. D*. 1989, **22**, 1185.
33 E. M Johannes, N. Klein and B. Plietker, *Org.biomol.chem.* 2013, **11,** 1271.
34J. Chastain and R. C. King, *Handbook of X-ray Photoelectron SpectroscopyPhysical Electronics. Inc. Eden Prairie.* 1995, 80.
35 R. V. Siriwardane and J. M Cook, *J. Colloid Interface Sci*. 1985, **108**, 414.
36 J. Chlistunoff, *J. Phys. Chem*. C. 2011.**115**, 6496.
37 H. Schulenburg, S. Stankov, V. Schunemann, J. Radnik, I. Dorbandt, S. Fiechter, P. Bogdanoff and H. Tributsch, *J. Phys.Chem. B*. 2003, **107**, 9034.
38 H. Peng, Z. Mo, S. Liao, H. Liang, L. Yang, F. Luo, H. Song, Y. Zhong and B. Zhang, *Scientific Reports.* 2013, **3**, 1765.
39 A. J. Bard and L. R. Faulkner, *Electrochemical Methods*, 2nd ed. John Wiley and Sons, New York, 2001.
40 H. Ye and R. M. Crooks, *J. Am. Chem. Soc*. 2007, **129**, 3627.
41 G. Zhang and F. Yang, *Electrochim. Acta*. 2007, **52**, 6595.
42 X. Fu , Y. Liu Y, X. Cao, J. Jin, Q. Liu and J. Zhang, *Appl Catal B Environ.* 2013, **130**, 143.
43 K. Niu, B. Yang B, J. Cui, J. Jin, X. Fu, Q. Zhao and J. Zhang, *J. Power Sources.* 2013, **243**, 65.
44 S. Kuroki, Y. Hosaka, C. Yamauchi, M. Sonoda, Y, Nabae, M.A. Kakimoto and S. Miyata, *J Electrochem. Soc.* 2012, **159**, 309.
45Q. Dong, X. Zhuang, Z. Li, B. Li, B. Fang, C. Yang, H. Xie, F.Zhang, and X. Feng, *J. Mater. Chem. A*. 2015, **3**, 7767
46 J.Sanetuntikul and S.Shanmugam, *Nano Scale*. 2015, **7**, 7644

Table of Content

Here, we report a low-cost, noble metal free Fe-N-C catalyst prepared using carbonized polyaniline (PANI) and ferric chloride as precursors in an inert atmosphere for oxygen reduction reaction.